

Flux Attenuation due to Sensor Displacement over Sea

ERIK O. NILSSON AND ANNA RUTGERSSON

Department of Earth Sciences, Uppsala University, Uppsala, Sweden

PETER P. SULLIVAN

National Center for Atmospheric Research, Boulder, Colorado

(Manuscript received 4 September 2009, in final form 13 January 2010)

ABSTRACT

When using the eddy correlation method to measure turbulent scalar fluxes, there is often a spatial separation between the instruments measuring the scalar and the vertical velocity. The attenuation of the flux due to this separation is studied here for marine conditions. Measurements of a two-point covariance between vertical velocity and temperature are compared to covariance measurements from collocated sensors for both horizontal and vertical displacements, with the purpose of finding the approximate functions to describe the flux loss for typical separation distances. On the basis of this study's measurements, there is only a slight directional dependence (i.e., streamwise or crosswind separation) of the flux loss for sensor separation distances less than 1 m but an increasing dependence with increasing displacement distance. For a vertical displacement, observations from this study confirm that flux loss is less with the scalar sensor positioned below the velocity sensor than at an equal distance above. Furthermore, the data show a clear dependence on atmospheric stability with increasing flux loss for increasing stable stratification, but it is not as large as that found in previous studies of flux attenuation over land. For example, the authors compare estimated flux loss for neutral and moderately stable ($z/L = 0.3$) stratification at a measuring height of $z = 10$ m and a sensor displacement $r = 0.3$ m, where L is the Obukhov length. For neutral (stable, $z/L = 0.3$) stratification the estimated loss of flux is 3% (5%) of the total flux for horizontal displacement. Whereas for an equal vertical separation the estimates are 2% (4%) when the scalar sensor is placed above the anemometer but less than 1% (2%) if it is placed below. Thus, the authors conclude that placing the scalar sensor below the anemometer minimizes the flux loss due to sensor separation, and that a simple correction function can be used to quantify the mean flux loss due to sensor separation over sea.

1. Introduction

The eddy correlation method is a standard method to determine turbulent scalar fluxes. The method uses correlation of the high-frequency signal of the vertical velocity and the scalar of interest. If the two signals are measured by separate instruments (which is the case for many scalars), the sensors must be separated to avoid flow distortion. This displacement unfortunately attenuates the flux estimate. The loss of flux occurs because of an unavoidable decorrelation between velocity and scalar variables at small scales. The attenuation is a function of the ratio of the sensor displacement and the scale of the

turbulence (Kristensen et al. 1997). Various methods to account for sensor separation exist, such as in situ techniques (e.g., Villalobos 1997; Laubach and McNaughton 1998) requiring multiple sensors or various cospectral transfer function approaches (Moore 1986), correcting for the flux loss differently for different parts of the cospectra. These approaches require access to the individual raw data from the high-frequency sensors. Here, we instead investigate using a simple correction function approach to estimate the flux attenuation due to sensor separation. If the flux attenuation is known, the measured flux can be corrected by dividing it by the fractional attenuation.

The impact of sensor separation on scalar fluxes has been investigated previously in several studies (e.g., Lee and Black 1994; Kristensen et al. 1997; Horst and Lenschow 2009) using datasets of temperature and vertical velocity collected at land sites. Horst and Lenschow (2009) used data from the horizontal array turbulence study (HATS),

Corresponding author address: Erik O. Nilsson, Dept. of Earth Sciences, Uppsala University, Villavägen 16, 752 36 Uppsala, Sweden.
E-mail: erik.nilsson@met.uu.se

which was carried out at a flat terrain site in the San Joaquin Valley of Southern California. Kristensen et al. (1997) used data from two different locations: the Marshall field site near Boulder, Colorado, and the Risø Integrated Milieu project (RIMI) site near Roskilde, Denmark. The purpose of our study is to investigate the flux loss over sea using data from the ocean horizontal array turbulence study (OHATS), where the instrument setup is similar to HATS. The results for the observed attenuation of heat flux are assumed to apply for other scalar fluxes as well because of the scalar similarity (Hill 1989), although recent results suggest possible limitations of this concept, especially in the long-wave part of the spectrum (Ruppert et al. 2006). The influence from the diurnal cycle on scalar similarity is also discussed in Ruppert et al. (2006) based on measurements over grassland, an irrigated cotton plantation, and a spruce forest; however, no assessment of such effects has, to our knowledge, been carried out over sea, where the diurnal variation in heat flux is expected to be smaller.

Lee and Black (1994) conducted experiments in a potato field and a clover field in British Columbia, Canada, and found that displacing the scalar sensor in the mean wind direction (streamwise displacements are denoted r_x) results in less flux loss than displacing the sensor perpendicular to the mean wind direction (crosswind displacements are denoted r_y), whereas Kristensen et al. (1997) did not find a flow direction dependence. Horst and Lenschow (2009) conclude that the HATS data support a model of wind direction dependence similar to that of Lee and Black (1994) and argue that Kristensen et al. (1997) found no wind direction dependence because of their limited range of data. Kristensen et al. (1997) examined mostly unstable stratification and separation distances $r/z \leq 0.25$, where r is the distance between the sensors, and z is the height above the surface.

Lee and Black (1994) derived an expression for flux attenuation based on a flux cospectrum suggested by Wyngaard and Coté (1972). The attenuation is then a function of $(r/z)^{4/3}$ as can be argued by dimensional analysis. Horst and Lenschow (2009) did not find support for this dependence using the HATS data and argue by theoretical analysis that a dependence on $(r/z)^{4/3}$ only applies for very small values of r/z . Horst and Lenschow (2009) instead adopt a cospectrum model for crosswind displacements, which departs from the theoretical inertial range slope of $-7/3$ but is found to provide a close match to the Kansas stable streamwise cospectra of Kaimal et al. (1972). The shape of the cospectrum leads to a simple exponential correction describing flux loss.

No previous study has analyzed the attenuation of scalar fluxes over sea. Horst and Lenschow (2009) state that the HATS flux attenuation relations “are not valid

where the dependence on wavenumber of the scalar-flux cospectrum differs materially from that in the terrestrial surface-flux layer,” and that this is likely to be true for measurements over sea. The present paper attempts to address this issue and quantify the flux loss due to sensor separation over sea. The goal of our study is to find approximate functions describing flux loss for typical separation distances in the marine atmospheric surface layer. Flux attenuation is investigated for three principal directions: sensor separation in the mean wind direction r_x , that is, separation in the streamwise direction; crosswind sensor separation r_y , that is, separation perpendicular to the mean wind direction; and also vertical sensor separation.

The topic of flux attenuation due to vertical sensor displacement is also examined in Kristensen et al. (1997) and Horst and Lenschow (2009). Both of these studies arrive at the unexpected result that the flux attenuation is less when the scalar sensor is placed below the velocity sensor rather than above. This result will be tested using the two vertically separated arrays of sonic anemometers deployed during OHATS.

2. Theory

Flux attenuation models are based on a theoretical relationship for the cross covariance between two parameters with a spatial displacement:

$$\overline{w'(\mathbf{x})\theta'(\mathbf{x} + \mathbf{r})} = \iiint_{-\infty}^{\infty} \Phi_{w\theta}(\mathbf{k})e^{i\mathbf{k}\cdot\mathbf{r}} d^3\mathbf{k} \quad (1)$$

(e.g., Lumley and Panofsky 1964, section 1.13). Here, $\mathbf{r} = (r_x, r_y, r_z)$ denotes the spatial displacement vector, $\mathbf{x} = (x, y, z)$ denotes the position vector, $\mathbf{k} = (k_x, k_y, k_z)$ is the three-dimensional wavenumber vector, and $\Phi_{w\theta}(\mathbf{k})$ is the three-dimensional cross spectrum between vertical velocity and temperature density fluctuations at the same location.

For a horizontal displacement $\mathbf{r} = (r_x, r_y, 0)$ we follow the nomenclature of Horst and Lenschow (2009) introduced in their Fig. 1 and define k_1 as the wavenumber parallel to a horizontal spatial displacement, that is, $\mathbf{k} \cdot \mathbf{r} = k_x r_x + k_y r_y \equiv k_1 r$. For the above relationship we can then write

$$\overline{w'(x, y, z)\theta'(x + r_x, y + r_y, z)} = \int_{-\infty}^{\infty} \text{Cr}_{w\theta}(k_1)e^{ik_1 r} dk_1, \quad (2)$$

where $\text{Cr}_{w\theta}(k_1)$ is the complex one-dimensional cross-spectrum along k_1 , which can be separated into real and imaginary parts:

$$Cr_{w\theta}(k_1) = \iint_{-\infty}^{\infty} \Phi_{w\theta}(\mathbf{k}) dk_2 dk_3 = Co_{w\theta}(k_1) - iQ_{w\theta}(k_1), \quad (3)$$

where $Co_{w\theta}(k_1)$ and $Q_{w\theta}(k_1)$ are the one-dimensional cospectrum and quadrature spectrum, respectively.

Substituting Eq. (3) into Eq. (2) and dividing by the collocated flux F_0 , an expression for the flux attenuation is obtained,

$$\begin{aligned} \frac{\overline{w'(\mathbf{x})\theta'(\mathbf{x}+\mathbf{r})}}{\overline{w'(\mathbf{x})\theta'(\mathbf{x})}} &= \frac{F(\mathbf{r})}{F_0} \\ &= \frac{1}{F_0} \int_{-\infty}^{\infty} [Co_{w\theta}(k_1) - iQ_{w\theta}(k_1)] e^{ik_1 r} dk_1. \end{aligned} \quad (4)$$

Similar to Horst (2006), it is assumed that $Q_{w\theta}(k_1) \ll Co_{w\theta}(k_1)$, and then Eq. (4) can be rewritten as

$$\frac{F(\mathbf{r})}{F_0} = \frac{1}{F_0} \int_{-\infty}^{\infty} Co_{w\theta}(k_1) \cos(k_1 r) dk_1. \quad (5)$$

The procedure followed in Horst and Lenschow (2009) as well as Kristensen et al. (1997) is to adopt a cospectrum model and then integrate it to obtain a quantitative description of the flux attenuation. Generally, this integration must be done numerically but in specialized cases it can be done analytically. The exponential model from Horst and Lenschow (2009) is such a case.

By assuming a cospectrum of the form

$$Co_{w\theta}(k_1) = \frac{2}{\pi k_m \left[1 + \left(\frac{k_1}{k_m} \right)^2 \right]}, \quad (6)$$

which corresponds to a Cauchy–Lorentz distribution, Horst and Lenschow (2009) integrate Eq. (5) and obtain the exponential model

$$\frac{F(r)}{F_0} = e^{-k_m r} \quad (7)$$

for flux attenuation, where k_m is the wavenumber at the maximum of the frequency-weighted cospectrum.

Horst (1997) finds that Eq. (6) is a close match to the Kansas stable streamwise cospectra of Kaimal et al. (1972), and the corresponding exponential model for the flux loss, Eq. (7), was used in Horst and Lenschow (2009) to describe flux attenuation. For all cases, except for streamwise sensor displacement during unstable stratification, Horst and Lenschow (2009) find that the simple model of

Eq. (7) can be used to approximate the measured flux loss, when the wavenumber of the cospectral peak k_m is parameterized as a function of stability z/L , where L is the Monin–Obukhov length $L = -u_*^3 T_0 / g \kappa w' \theta'_v$. Here, u_* is the friction velocity; $w' \theta'_v$ is the kinematic virtual heat flux; θ_v is the virtual temperature; $\kappa = 0.4$ is the von Kármán constant; and g/T_0 is the buoyancy parameter, where T_0 is the average boundary layer temperature and g is the acceleration of gravity. Negative and positive values of z/L refer to unstable and stable stratification, respectively.

For unstable stratification Horst and Lenschow (2009) instead find that the flux attenuation for streamwise sensor displacement is estimated quite well by the integral of an adopted cospectral formula:

$$\frac{F(r_x)}{F_0} = A(\mu) \int_{-\infty}^{\infty} \frac{\cos(k_{xm} r_x k')}{(1 + 0.75 k'^{2\mu})^{7/6\mu}} dk', \quad (8)$$

originally developed by Kristensen et al. (1997) as a circular symmetric model to apply in all horizontal directions under the assumption of a negligible quadrature spectrum. Here, $k' = k_x/k_{xm}$, k_{xm} is the wavenumber at the maximum of the wavenumber-multiplied cospectrum for the wavenumber parallel to r_x , and k_x is the wavenumber along the mean wind direction. In Horst and Lenschow (2009), both μ , a parameter describing the shape of the cospectra, and k_{xm} are stability-dependent parameters. Equation (8) is integrated numerically to obtain estimates of the flux attenuation for streamwise sensor displacements.

In general, a horizontal displacement is composed of both streamwise and crosswind displacements, and Horst and Lenschow (2009) suggest a simple model for an arbitrary horizontal sensor displacement of the form

$$\frac{F(r)}{F_0} = e^{-(\ln^2 A_x + \ln^2 A_y)^{1/2}}. \quad (9)$$

Here, A_x and A_y are models of the ratio between displaced and collocated covariance for streamwise and crosswind displacement. In the HATS flux attenuation model described in Horst and Lenschow (2009), $A_y = F(r_y)/F_0$ was determined by Eq. (7), and $A_x = F(r_x)/F_0$ was determined by numerical integration of the cospectral formula of Eq. (8). This model is found to be in agreement with the measured flux loss using the HATS dataset.

An alternative approach to Eq. (8) is also suggested in Horst and Lenschow (2009). First, account for streamwise sensor separation using Taylor's hypothesis—that is, simply lag the data from the upstream sensor by the time difference required to maximize the correlation

between w' and c' . Then, Eq. (9) reduces to Eq. (7) and one only needs to correct for crosswind sensor separation.

Horst (2006) also explored the possibility of using Eq. (9) with $A_x = F(r_x)/F_0 = e^{-k_m r_x}$ and $A_y = F(r_y)/F_0 = e^{-k_m r_y}$, that is, with both A_x and A_y determined by Eq. (7). It was found that, for flux attenuation less than about 40%, Eq. (9) was a good approximation for all wind directions (Horst 2006).

In the present investigation, we suggest an alternative distribution called a Voigt profile, which allows us to account for additional processes contributing to the flux. The Voigt profile is used in spectroscopy (e.g., section 3.2 of Demtröder 2003; Armstrong and Nicholls 1972; Pagnini and Saxena 2008, manuscript submitted to *J. Phys. A: Math. Gen.*, available online at http://arxiv.org/PS_cache/arxiv/pdf/0805/0805.2274v1.pdf) to describe the shape of spectra when there are influences from two mechanisms: one of which produces a Gaussian profile, and the other produces a Cauchy–Lorentz profile. The Voigt profile is the convolution of Gaussian and Cauchy–Lorentz profiles and can be expressed as the real part of the complex error function:

$$Co_{w\theta}(k_1) = \frac{1}{\sqrt{\pi k_b}} \text{Re}[e^{z^2} \text{erfc}(z)], \quad (10)$$

where $z = (k_a + ik_1)/(2\sqrt{k_b})$, k_a and k_b are two positive constants, and $\text{erfc}(z)$ is the complementary complex error function. By assuming a cospectrum of this form the integration can still be done analytically, but it leads to a new modified exponential model for the flux attenuation:

$$\frac{F(r)}{F_0} = e^{-k_a|r| - k_b r^2}. \quad (11)$$

This new functional form also provides another fitting parameter, that is, k_b , which allows us to better fit our observational data.

3. Site description and measurements

The data used in this investigation are from the field campaign OHATS carried out at the air–sea interaction tower (ASIT). The location of the ASIT is south of Martha’s Vineyard on the East Coast of the United States. The tower is located in water at a depth of about 15 m and carries a specially configured rack consisting of twin radio tower sections designed and built to hold two horizontal booms. On each boom nine sonic anemometers were mounted with a separation distance of 0.58 m. The two horizontal booms were deployed at a nominal height of 5 and 5.58 m above the mean sea surface; see Figs. 1 and 2. The heights were chosen to capture as

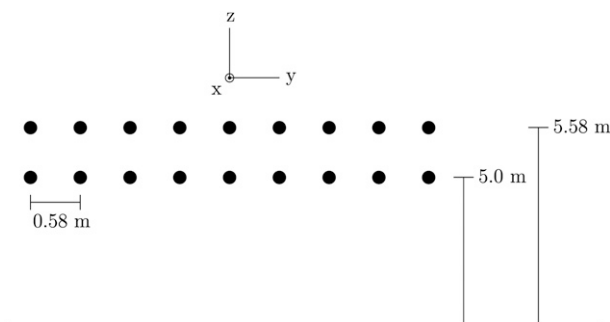


FIG. 1. Two arrays with nine sonic anemometers each at nominal heights 5 and 5.58 m above mean sea level with a horizontal separation distance of 0.58 m. The circled dot in the sketch of the x – y – z coordinate system indicates the streamwise x axis being directed out of the plane of the page.

much of the turbulence characteristics associated with air–sea interaction as possible but, on the other hand, avoid swamping the instrumentation (Sullivan et al. 2006). The rack is located upwind of the ASIT to avoid interference from the tower legs. The sonic anemometers used to measure winds and temperature were Campbell Scientific anemometers (CSAT3) with a sampling frequency of 20 Hz.

Wave measurements were available for most of the period analyzed in this study. They were collected using three downward-pointing Riegel laser altimeters mounted beneath the ASIT diving board in a triangular pattern with 2-m horizontal spacing. This configuration allows measurement of wave amplitude and propagation direction, and it also provides information about the phase speed of the dominant wave. A further description of the OHATS field campaign and the ASIT research platform can be found in Sullivan et al. (2006) or at the Web site for OHATS (2009; available online at <http://www.whoi.edu/science/AOPE/dept/OHATS/intro.html>). The measurements were taken during the 7 August to 18 October 2004 period. The data have been subjectively filtered and periods with large variability between individual sonic measurements have been removed—these data are assumed to be severely influenced by flow distortion or other disturbances. Each 30-min period has also undergone a visual quality control by the examination of individual cospectra of sensible heat flux. Shown in Fig. 3 is the mean cospectral behavior for different intervals of the stability parameter z/L . Here, T_* is the characteristic temperature for the surface layer. There is a clear shift toward higher frequencies for the more stable cospectra.

The data are also filtered with respect to mean wind direction to only include periods with wind directions in a range of $\pm 38^\circ$ normal to the array. Periods with near-neutral stratification, $|z/L| < 0.015$, associated with small heat fluxes are removed as well as periods with wind

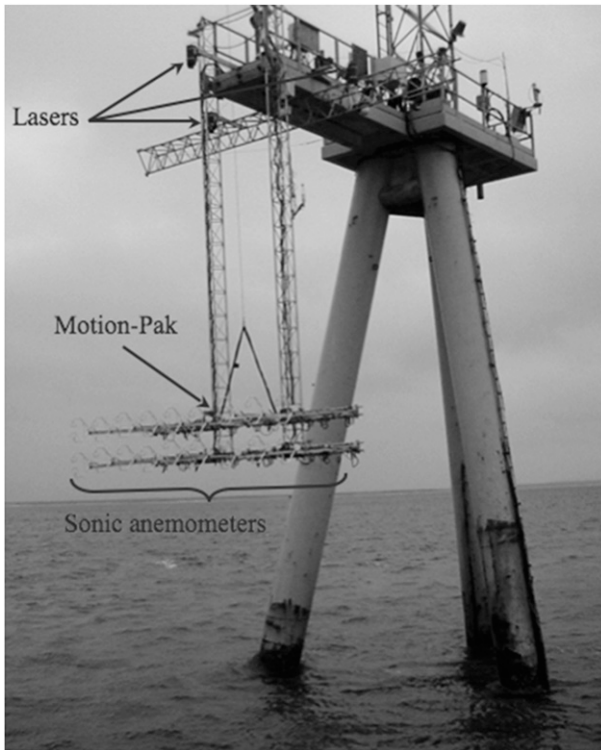


FIG. 2. The instrumental setup and the air–sea interaction tower during OHATS adapted from Sullivan et al. (2006).

speed U lower than 2.5 m s^{-1} . This procedure leaves a dataset consisting of 191 periods, each 30 min long. This subset of the OHATS database covers a wide range of atmospheric stability conditions, $-1.0 < z/L < 1.4$, with wind speed U up to 12.8 m s^{-1} . Sea level variations give a varying measuring height between 4.1 and 5.5 m for the lowest array.

The measured flux loss is defined as the ratio of displaced and collocated covariance $F(r)/F_0$. For each height, separation distance, and half-hour of data analyzed in this study, the flux loss ratio $F(r)/F_0$ is determined by the slope a of a fitted line between displaced and collocated covariance:

$$a = \frac{\sum_{i=1}^N F_i(r)}{\sum_{i=1}^N F_i(0)}.$$

For one array of nine equidistant displaced sonic anemometers there are a total of 16 horizontally displaced fluxes for the smallest separation distance, but there are only 2 for the longest separation distances. The two vertically separated arrays allowed for a total of nine vertically displaced fluxes with the scalar sensor placed below (as well as above) the sonic anemometer.

4. Results

A general sensor separation can be decomposed into streamwise, crosswind, and vertical separation, each with a possible contribution to the total flux loss. As previously mentioned, flux loss due to streamwise sensor separation can be taken into account by using Taylor's hypothesis. For crosswind or vertical sensor separation there is no similar approach, and hence we need to determine the flux loss from multipoint measurements. Horst and Lenschow (2009) suggest Eq. (9) as a generalized formula for a horizontal sensor displacement (separation in the x - y plane). We instead determine flux attenuation due to streamwise separation by maximizing the correlation between w' and c' and then add corrections due to crosswind and vertical separations. Equation (9) is then rewritten as

$$\frac{F(\mathbf{r})}{F_0} = e^{-(\ln^2 A_y + \ln^2 A_z)^{1/2}}. \quad (12)$$

Here, A_y and A_z are models of the ratio between displaced and collocated covariance for crosswind and vertical displacements. To use Eq. (12), we need to determine A_y and A_z from measurements, as described in sections 4a and 4c, respectively. We also investigate the OHATS dataset for streamwise flux loss in section 4b. In all cases, we have taken the sea level variations into account by using z equal to the individual height of each array above sea level for each 30-min period of data analyzed. The nominal heights of 5 and 5.58 m above mean sea level for the two arrays were used only for 26 cases at the beginning of the measurement period, when wave measurements were not available.

a. Crosswind sensor separation

The fluxes for crosswind sensor separation were calculated following the procedure in Horst and Lenschow (2009) by first projecting the OHATS data from each of the two arrays onto lines perpendicular to the mean wind direction. This can be done by delaying the data from each sonic anemometer by a different time lag dependent on wind speed and wind direction, for details see Horst and Lenschow (2009).

Figure 4 shows flux loss due to crosswind displacement as a function of stability. The errorbars denote ± 1 standard deviation from the averages over each stability interval. The OHATS crosswind flux-loss data are fitted to Eq. (11), resulting in the empirical formulas for A_y in Eq. (12):

$$\text{for } z/L \leq 0$$

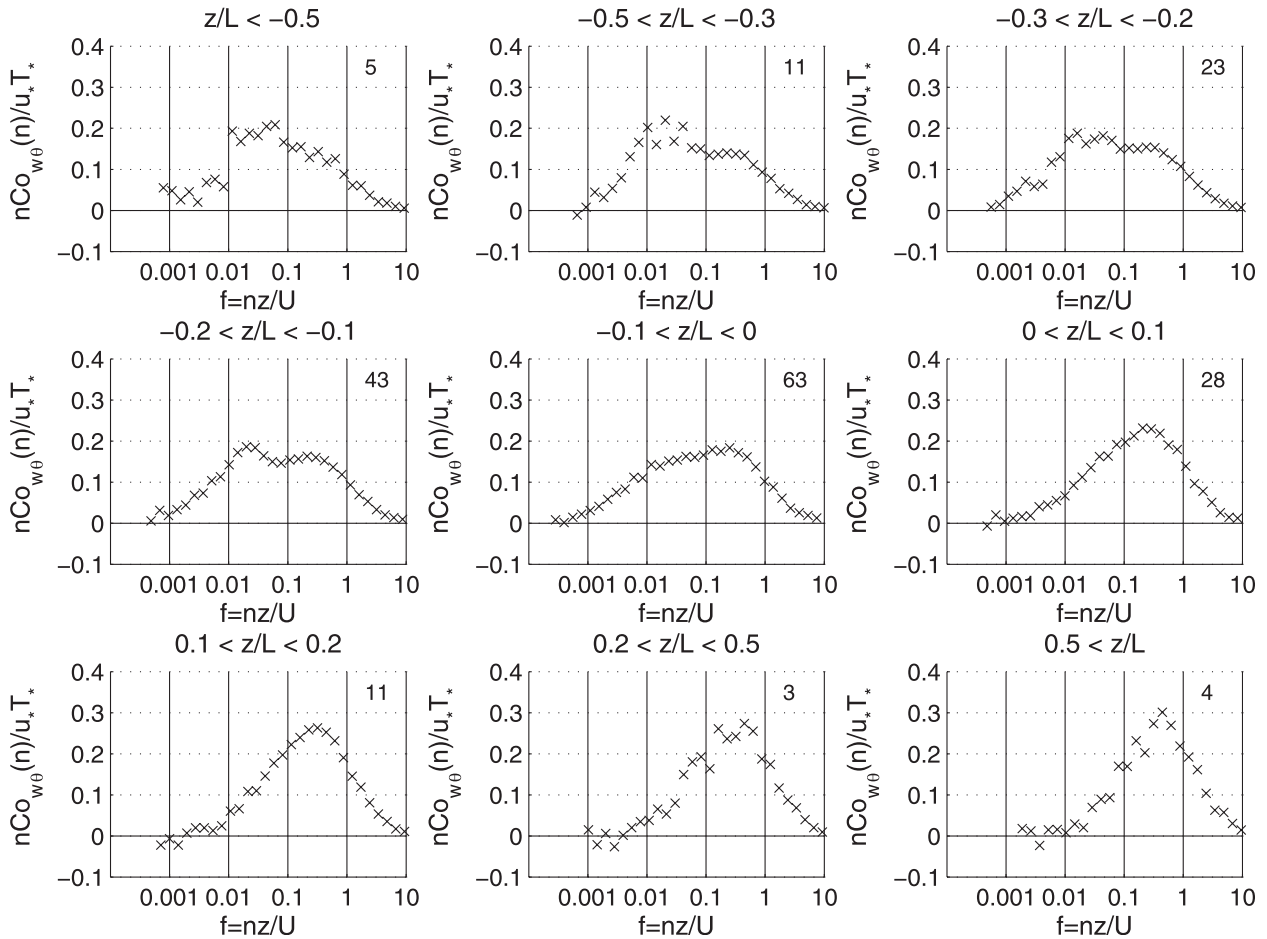


FIG. 3. Normalized mean streamwise cospectra of sensible heat flux for different stability intervals. The number in the upper right corner represents the number of half-hours used for each stability interval.

$$A_{13} = \frac{F(r_y)}{F_0} = e^{-\left(0.38 + \frac{0.01}{0.04 - z/L}\right)\left(\frac{r_y}{z}\right)^2 - \left(0.62 + \frac{0.014}{0.04 - z/L}\right)\left(\frac{r_y}{z}\right)}, \quad (13)$$

and for $z/L > 0$

$$A_{14} = \frac{F(r_y)}{F_0} = e^{-\left(4.53 - \frac{3.9}{1 + (z/L)^{3/4}}\right)\left(\frac{r_y}{z}\right)^2 - \left(2.87 - \frac{1.9}{1 + (z/L)^{3/4}}\right)\left(\frac{r_y}{z}\right)}. \quad (14)$$

The black lines with circles, crosses, and dots shown in Fig. 4 correspond to the predictions of these functions for three different values of the nondimensional ratio r_y/z . Also shown are the correction functions of Horst and Lenschow (2009) as gray lines. The attenuation calculated with the expression from Horst and Lenschow (2009) is larger than the present data for unstable stratification

and increases more with increasing z/L than the present data. This indicates that the flux loss due to crosswind sensor displacement is less in the OHATS dataset (over sea) as compared to the HATS dataset (over land), and that the largest differences are seen for increasing stable stratification.

The analysis of measured crosswind flux loss in Fig. 5 shows that the estimation of flux attenuation due to crosswind sensor separation by a function of the form $F(r_y)/F_0 = e^{-2\pi n_{my} r_y/z}$ (Horst and Lenschow 2009) do not agree with our measured data representing marine conditions. The attenuation coefficient n_{my} in their formulation is required to be independent of the normalized separation distance r_y/z , and this is not valid over sea. Figure 5 illustrates this by showing values of the attenuation normalized by height above actual sea level and separation distance $-z \ln[F(r_y)/F_0]/2\pi r_y$ calculated from measurements for four different intervals of r_y/z . The dashed lines in Fig. 5 correspond to the expression from Lee and Black (1994):

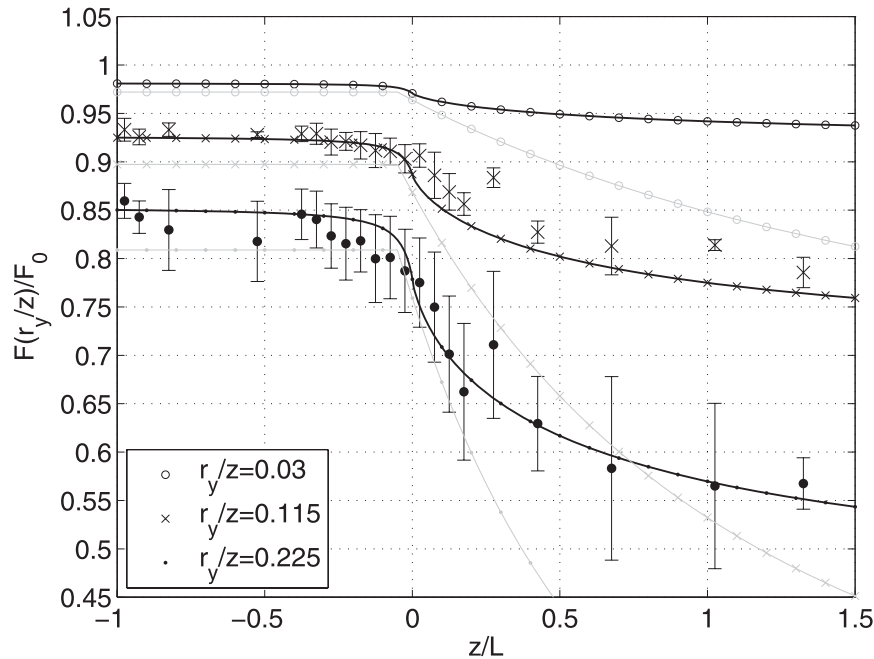


FIG. 4. Estimated and bin-averaged crosswind flux loss for different values of r_y/z (thick markers with error bars). Error bars represent one standard deviation from bin-averaged values for half-hours with r_y/z in the intervals 0.08–0.15 and 0.15–0.30, respectively. The thick black lines with circles, crosses, and dots correspond to Eqs. (13)–(14) for three values of r_y/z . The thinner gray lines with circles, crosses, and dots correspond to the correction function proposed by Horst and Lenschow (2009) for the same values of r_y/z .

$$\frac{F(r)}{F_0} = e^{-\alpha \phi_h \phi_\epsilon (r/z)^{4/3}}. \quad (15)$$

The wind direction dependent coefficient α in Eq. (15) corresponds to values found by Lee and Black (1994) for crosswind sensor separation and unstable stratification. Here, ϕ_h and ϕ_ϵ are the same universal functions for sensible heat and energy dissipation that Lee and Black (1994) used for unstable stratification. For stable stratification we have used an extrapolation of their formula but replaced the similarity functions ϕ_h and ϕ_ϵ with corresponding formulas for stable stratification, $\phi_h = 1 + 8.0z/L$ from Höögström (1996) and $\phi_\epsilon^{2/3} = 1 + 2.5|z/L|^{3/5}$ from Kaimal et al. (1972).

Figure 5 shows that Eqs. (13)–(14) generally provide a better estimate of flux loss than the correction functions from Horst and Lenschow (2009) or Lee and Black (1994) for the present data. This is especially true for increasing stable stratification, largely owing to the additional squared term in the exponent of Eq. (11).

Horst and Lenschow (2009) argue that theoretically the dependence on $(r/z)^{4/3}$ used by Lee and Black (1994) applies only for separation distances much smaller than those analyzed here. From Fig. 5 there is a noticeable increase in the measured values of the normalized

attenuation $\{-z \ln[F(r_y)/F_0]/2\pi r_y\}$ with increasing r_y/z . An increase of the normalized attenuation with increasing r_y/z is also suggested by the expression from Lee and Black (1994; see dashed lines in Fig. 5). Horst and Lenschow (2009) also note that a model $F(r_y)/F_0 = e^{-(k_m r_y)^b}$ can provide a better fit to their data with b varying from 1.09 for unstable stratification to 1.22 for stable stratification, which corresponds to a varying normalized attenuation with varying r_y/z as is suggested here.

b. Streamwise sensor separation

The attenuation due to streamwise sensor separation was estimated by assuming Taylor's hypothesis (see section 2). The advection velocity was estimated to be the mean wind speed, although we do note that the speed at which turbulent structures are being advected relates to eddy size, with small eddies being advected at the local wind speed, while large eddies are advected at greater speed (Horst and Lenschow 2009). During the HATS campaign, additional tower measurements could be used to investigate the advection velocity, but over sea during OHATS no such advection tower measurements were performed. Tests of changing the advection velocity to 1.1 times the mean wind speed, as suggested from the HATS

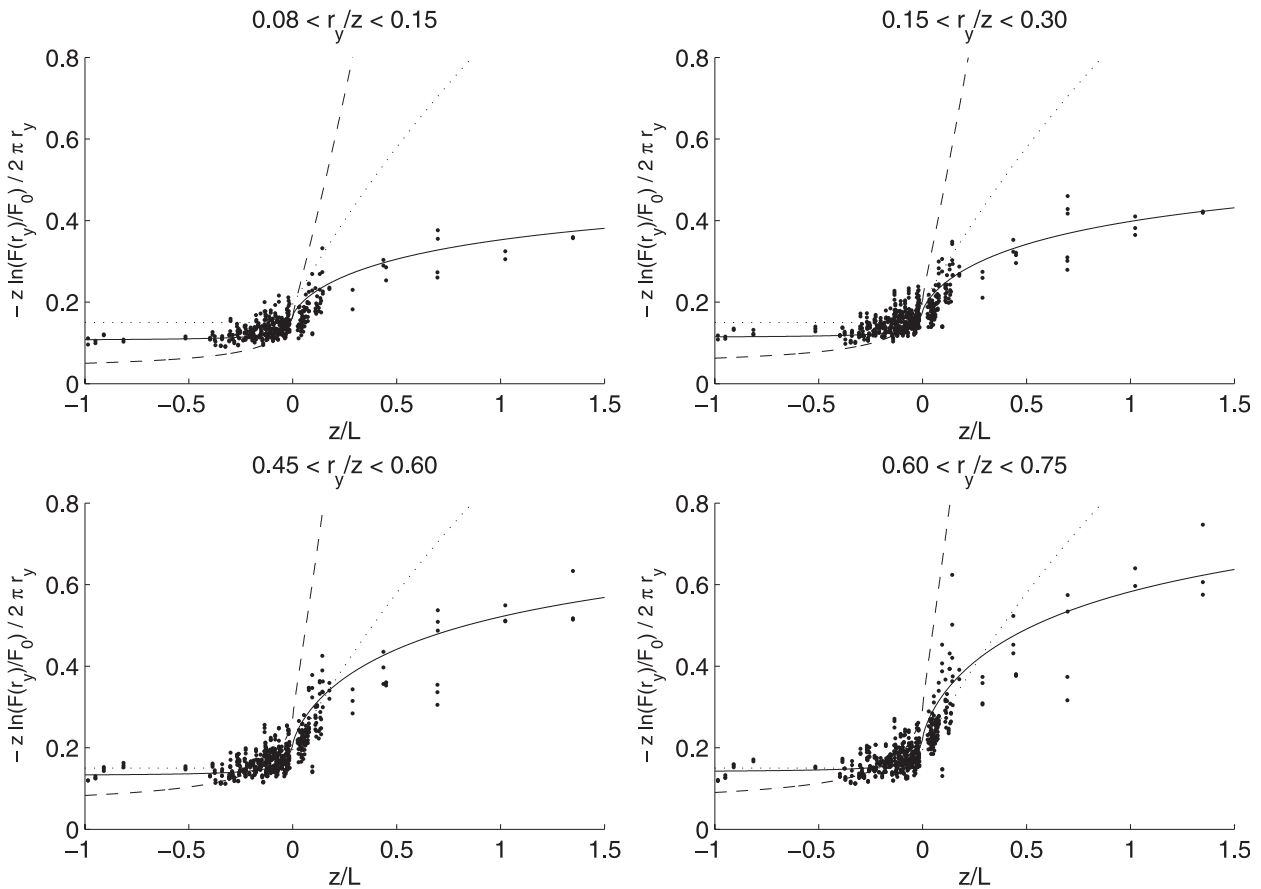


FIG. 5. Normalized attenuation due to crosswind sensor displacement as a function of stability for different ranges of r_y/z . The black dots are the OHATS data. The full line shows the normalized flux-loss estimate from Eqs. (13)–(14). The empirical formula from Horst and Lenschow (2009) is shown as the dotted line and the dashed line shows the normalized flux-loss estimate from Lee and Black (1994) for unstable conditions, with an extrapolation of their expression to stable conditions.

data Horst and Lenschow (2009), only gave minor effects on estimates of flux loss because of the typically small sensor separation.

Figure 6 shows flux loss as a function of stability. Displaced time series with the temperature sensor upwind and downwind of the sonic anemometer are used to compute the mean values and standard deviations for each z/L interval. Only small differences were found with the scalar sensor upwind or downwind of the sonic during unstable stratification. For stable stratification the differences were slightly larger, with less flux loss for the scalar sensor located upwind of the velocity measurement. These differences between upwind and downwind displacements are possibly related to the behavior of the quadrature spectrum (T. Horst 2008, personal communication). The quadrature spectrum enters into Eq. (4), but it is usually assumed to be small in comparison to the cospectrum and is neglected. For streamwise sensor displacement, no clear dependence on separation distance for varying normalized attenuation is observed (not shown here).

Consequently, a separate “squared term” as is used for crosswind sensor separation is not needed. For the purpose of finding an approximate correction function it is therefore convenient to use a function of the form similar to Eq. (7) for streamwise sensor separation.

The OHATS streamwise flux-loss data are fitted to Eq. (7) with the empirical formulas:
for $z/L \leq 0$

$$\frac{F(r_x)}{F_0} = e^{-\left(0.65 + \frac{0.014}{0.04 - z/L}\right)\left(\frac{r_x}{z}\right)}, \tag{16}$$

and for $z/L > 0$

$$\frac{F(r_x)}{F_0} = e^{-\left(3.5 - \frac{2.5}{1 + (z/L)^{3/4}}\right)\left(\frac{r_x}{z}\right)}. \tag{17}$$

The black lines with circles, crosses, and dots shown in Fig. 6 correspond to these functions for three different values of the nondimensional ratio r_x/z .

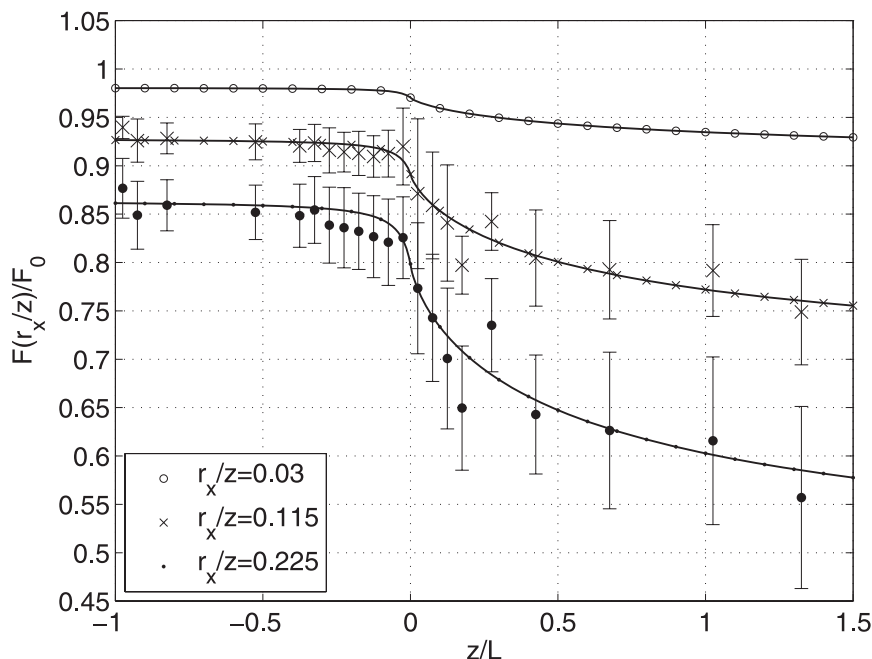


FIG. 6. Estimated and bin-averaged streamwise flux loss for different values of r_x/z (thick markers with error bars). Error bars represent one standard deviation from bin-averaged values for half-hours with r_x/z in the intervals 0.08–0.15 and 0.15–0.30, respectively. The lines with circles, crosses, and dots correspond to Eqs. (16)–(17) for three values of r_x/z .

Lee and Black (1994) as well as Horst and Lenschow (2009) show that the flux loss is dependent on the wind direction relative to the displaced instruments, with less flux loss when instruments were separated in the mean wind direction (streamwise displacement); this is possibly because of elongation of turbulent eddies due to mean wind shear (e.g., Horst and Lenschow 2009; Nicholls and Readings 1981). Kristensen et al. (1997) did not find any significant dependence on wind direction and suggested a circular symmetric model for the flux loss due to horizontal displacement. Figures 4 and 6 suggest that there is only slight wind direction dependence when instruments are separated less than about 1 m (approximately $r/z < 0.2$ for our data). These separation distances are typically used for measuring scalar fluxes. A more careful comparison of flux loss due to crosswind and streamwise sensor separation for larger sensor displacements reveals, however, a difference between these two principal directions; the flux loss is less when instruments are separated in the mean wind direction. This is indicated by the slightly higher values of $F(r_x/z)/F_0$ in Fig. 6 in comparison to $F(r_y/z)/F_0$ in Fig. 4 for r_x/z and r_y/z in the interval 0.15–0.30. The difference between the directions is larger for larger sensor displacements. Data for larger displacement distances are not shown here because our focus is on the shorter separation distances, which are typical

separation distances between scalar and velocity sensors used in most studies of turbulent scalar fluxes.

c. Vertical sensor separation

The analysis of flux attenuation due to the vertical separation of instruments in this study is limited, because the two vertically separated arrays of sonic anemometers are nominally fixed at heights of 5 and 5.58 m above mean sea level during the OHATS field campaign. Sea level variations, however, cause the measuring height to vary between 4.1 and 5.5 m for the lower array. Kristensen et al. (1997) found little dependence on atmospheric stability for attenuation due to vertical separation and thus used only the ratio z/z' to describe the height dependence of the flux attenuation. Here, z and z' denote the measuring height of the velocity and scalar sensor, respectively. Horst and Lenschow (2009) did find a clear dependence on atmospheric stability and compared a generalization of the linear model from Kristensen et al. (1997) with an exponential model of the same form as Eq. (7). They find the exponential model to better represent their data. We use an exponential model of the same form as Eq. (7).

Figure 7 shows bin-averaged flux loss due to vertical displacement as a function of z_{\min}/L , where z_{\min} is the smaller of z and z' . It is observed that there is a dependence on stability with a larger flux loss for increasing

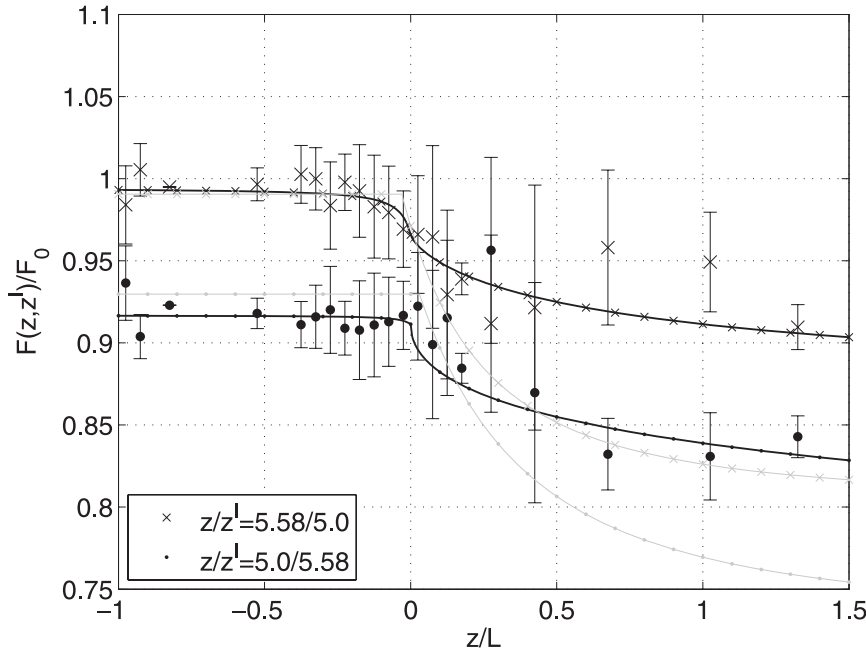


FIG. 7. Estimated and bin-averaged vertical flux loss for different values of z/z' (thick markers with error bars). Error bars represent one standard deviation from the bin-averaged values using all 191 30-min periods with z/z' in the intervals 1.10–1.15 and 0.87–0.91. The thick black line with dots shows the correction from Eqs. (18)–(19) for a scalar sensor 0.58 m above the vertical velocity measurement. The thick black line with crosses shows the correction from Eqs. (20)–(21) for a scalar sensor 0.58 m below the vertical velocity measurement. The estimated flux losses using the model from Horst and Lenschow (2009) are the thin gray lines with dots and crosses.

stable stratification. The OHATS vertical flux-loss data are fitted to the empirical formulas A_{18} – A_{21} for A_z in Eq. (12):

for $z_{\min}/L \leq 0$ with the scalar sensor above the sonic anemometer ($z/z' \leq 1$)

$$A_{18} = \frac{F(z, z')}{F_0} = e^{-\left(0.75 + \frac{0.002}{0.04 - z_{\min}/L}\right)\left(\frac{|z - z'|}{z_{\min}}\right)}, \quad (18)$$

and for $z_{\min}/L > 0$

$$A_{19} = \frac{F(z, z')}{F_0} = e^{-\left(3.3 - \frac{2.5}{1 + 0.4(z_{\min}/L)^2}\right)\left(\frac{|z - z'|}{z_{\min}}\right)}, \quad (19)$$

whereas for $z_{\min}/L \leq 0$ with the scalar sensor below the sonic anemometer ($z/z' > 1$)

$$A_{20} = \frac{F(z, z')}{F_0} = e^{-\left(0.05 + \frac{0.01}{0.04 - z_{\min}/L}\right)\left(\frac{|z - z'|}{z_{\min}}\right)}, \quad (20)$$

and for $z_{\min}/L > 0$

$$A_{21} = \frac{F(z, z')}{F_0} = e^{-\left(1.3 - \frac{1}{1 + (z_{\min}/L)^{3/4}}\right)\left(\frac{|z - z'|}{z_{\min}}\right)}. \quad (21)$$

The thick black lines with dots or crosses in Fig. 7 show the calculated vertical flux attenuation for typical measuring heights during OHATS. Error bars denote ± 1 standard deviation from the averaged measured values for different stability intervals. Flux loss using the model from Horst and Lenschow (2009) is also shown as thin gray lines with dots or crosses for the same values of z/z' .

The results displayed in Fig. 7 suggest that the OHATS dataset under neutral and unstable stratification correspond relatively well to what was found in Horst and Lenschow (2009). For unstable to near-neutral stratification, our data with the scalar sensor placed below the anemometer agrees well with the formula from Kristensen et al. (1997, not shown here). When the scalar sensor is placed above the anemometer, our unstable and near-neutral data show a slightly larger flux loss compared to what is estimated by the correction function from Horst and Lenschow (2009) but slightly less than estimated by Kristensen et al. (1997). The present data show

a decrease with increasing z_{\min}/L for stable data, which was not seen in Kristensen et al. (1997) but is in qualitative agreement with findings from the HATS dataset (Horst and Lenschow 2009). As found previously for crosswind sensor separation, the largest differences in flux loss due to vertical sensor separation in the OHATS dataset as compared to the HATS dataset are seen for stable stratification. The attenuation calculated with the expression from Horst and Lenschow (2009) is significantly larger than the present data and increases with increasing z_{\min}/L , indicating less flux loss for vertical separation over sea (OHATS) during stable conditions as compared to over land (HATS).

5. Discussion

The most striking difference between the results found in this study and Horst and Lenschow (2009) is the large difference in flux loss found during stable stratification, suggesting that the attenuation due to sensor separation is less over the ocean as compared to over land. The largest differences in the shape of cospectra over land and over sea occur during unstable stratification, where we observe saddle-shaped cospectra in data over sea. They appear to be a dominant feature of the marine atmospheric surface layer and were observed in several previous investigations (e.g., Nicholls and Readings 1981; Smedman et al. 2007; Sahlée et al. 2008). Saddle-shaped cospectra occur during unstable conditions and are likely a consequence of large turbulent eddies with long correlation scales. Hence, the flux loss caused by sensor separation is minimal under these conditions.

For crosswind sensor displacement, we observe less flux loss than what was observed in the HATS dataset for short separation distances. For longer separation distances, the flux loss in this study is comparable to the HATS data. This is possibly because of a different distribution of cospectral energy between smaller and larger scales over sea as compared to over land. Figure 8 shows a schematic figure of normalized cospectras corresponding to the model cospectra Eq. (6) suggested by Horst and Lenschow (2009, dotted line) and our newly suggested model cospectra Eq. (10) (full line). With less energy at the smallest scales our new cospectrum model representing sea data accounts for less flux loss at small separation distances and more at larger separations compared to turbulent flows over land.

Based on the flux-loss damping coefficients in Fig. 5, we propose a new exponential correction function with an added squared term for crosswind sensor separation, Eq. (11). This allows us to account for both crosswind, Eqs. (13) and (14), and streamwise, Eqs. (16) and (17), sensor separation with only a slight wind direction

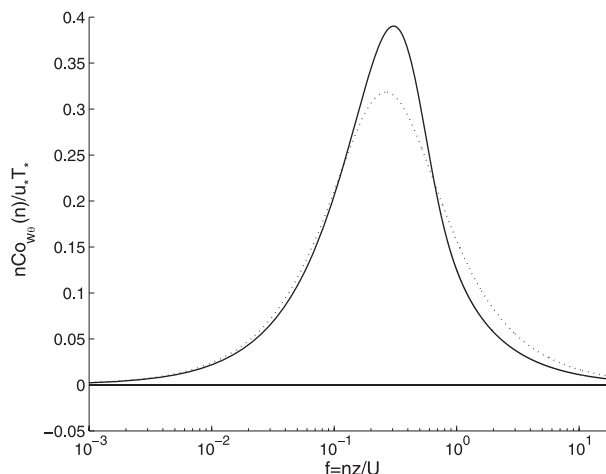


FIG. 8. Schematic of normalized crosswind cospectra from the model used in Horst and Lenschow (2009) shown as the dotted line [Eq. (6)], and from our newly suggested crosswind model shown as the solid line [Eq. (10)]. A different distribution of energy between smaller and larger scales is seen.

dependence at small separation distances—the dependence increases with larger displacements.

When investigating vertical displacement we found that flux loss due to sensor displacement is less when placing the scalar sensor below the sonic anemometer than with the scalar sensor above the anemometer or at an equal horizontal displacement. This is in agreement with Kristensen et al. (1997) and Horst and Lenschow (2009). This asymmetry is likely caused by the dependence of the vertical scalar gradient with height (Kristensen et al. 1997). No theoretical method to make a quantitative description of the flux loss caused by vertical separation has, however, been introduced, and we must therefore rely on empirical formulas. In addition to the vertical asymmetry, we also find a dependence on stability similar to what was found by Horst and Lenschow (2009), and we suggest a simple correction for the flux loss due to vertical sensor displacement over sea, Eqs. (18)–(21).

Observations of flux loss have also been investigated for varying wind speeds and states of the waves but no clear dependence was found. It is, however, not unlikely that dependencies related to the wave field would be possible to find at locations with a less-disturbed wave field. Other important issues that require further investigation are the validity of scalar similarity over ocean, and from a practical point of view, additional multipoint measurements with shorter separation distance between sensors would help improve our understanding of the effects of typical sensor displacement. The typical experimental setup for eddy-covariance measurements is the combination of one sonic anemometer with a fast-response temperature sensor and/or a fast-response gas

analyzer. For such a combination of sensors, typical sensor separation distances are about 0.1–0.3 m, that is, they are shorter than or at the lower edge of the range considered in this study.

6. Summary and conclusions

We analyze the attenuation of measured flux when using separate instruments for vertical wind and scalars. The data used in this investigation was collected in the marine atmospheric surface layer during the OHATS field campaign. We investigated the flux attenuation for the three principal directions of instrument separation and fit empirical formulas to the flux loss ratios $F(r_x)/F_0$, $F(r_y)/F_0$, and $F(z, z')/F_0$. In general, sensors can be separated in the mean wind direction r_x , normal to the mean wind direction r_y , as well as vertically.

Our recommendation on how to correct for flux attenuation over sea is to first account for streamwise sensor separation by using Taylor's hypothesis directly on the turbulence time series and simply lagging the data from the upstream sensor by the time difference required to maximize the correlation between w' and c' , as suggested in Horst and Lenschow (2009). Then, any additional correction for crosswind or vertical separation can be performed by applying Eqs. (13)–(14) and Eqs. (18)–(21) in the combined formula for horizontal sensor displacement as suggested by Horst and Lenschow (2009) but used in the y – z plane. Corrections for crosswind and vertical separation are given by $F(r)/F_0 = e^{-(\ln^2 A_y + \ln^2 A_z)^{1/2}}$, where A_y and A_z are empirical formulas describing flux loss due to crosswind and vertical sensor displacement, respectively. For unstable stratification, A_y is equal to A_{13} in Eq. (13) and for stable stratification A_y is equal to A_{14} from Eq. (14). In a similar way, for a scalar sensor located above the sonic anemometer, $A_z = A_{18}$ (A_{19}) for unstable (stable) stratification. With a scalar sensor placed below the sonic anemometer, A_z is equal to A_{20} (A_{21}) for unstable (stable) stratification.

As an example of our findings, compare the estimated flux loss for a fairly typical instrumental setup at a measuring height of $z = 10$ m with a sensor displacement $r = 0.3$ m between velocity and scalar sensors. For neutral (moderately stable, $z/L = 0.3$) stratification our results suggests a flux loss of 3% (5%) of the total flux if the sensor displacement is horizontal. If the sensors are vertically separated, our estimates indicate a flux loss of 2% (4%) when the scalar instrument is placed above the anemometer but less than 1% (2%) if it is placed below. We thus confirm the result found from previous studies over land (e.g., Kristensen et al. 1997; Horst and Lenschow 2009) that placing the scalar sensor below the anemometer minimizes the flux loss due to sensor separation.

Horst and Lenschow (2009) ask whether a simple correction function approach based on Monin–Obukhov similarity can be applied in a more complex situation such as the flow over a wavy sea surface. Although the scatter in the OHATS dataset is occasionally large, our results suggest that correction for attenuation is possible. We find that using simple correction functions are a convenient and accurate way of quantifying the mean flux loss due to sensor separation over sea.

Acknowledgments. We wish to thank Tom Horst at NCAR for valuable discussions concerning this work, and also the anonymous reviewers for many helpful comments and suggestions. Erik O. Nilsson is financed by the Swedish Research Council.

REFERENCES

- Armstrong, B., and R. Nicholls, 1972: *Emission, Absorption, and Transfer of Radiation in Heated Atmospheres*. Vol. 41, *International Series of Monographs in Natural Philosophy*, Pergamon Press, 295 pp.
- Demtröder, W., 2003: *Laser Spectroscopy: Basic Concepts and Instrumentation*. 3rd ed. Springer, 987 pp.
- Hill, R., 1989: Implications of Monin–Obukhov similarity theory for scalar quantities. *J. Atmos. Sci.*, **46**, 2236–2244.
- Högström, U., 1996: Review of some basic characteristics of the atmospheric surface layer. *Bound.-Layer Meteor.*, **78**, 215–246.
- Horst, T., 1997: A simple formula for attenuation of eddy fluxes measured with first-order-response scalar sensors. *Bound.-Layer Meteor.*, **82**, 219–233.
- , 2006: Attenuation of scalar fluxes measured with horizontally displaced sensors. Preprints, *17th Symp. on Boundary Layers and Turbulence*, San Diego, CA, Amer. Meteor. Soc., 7.5. [Available online at http://ams.confex.com/ams/BLTA/BioA/techprogram/paper_109629.htm.]
- , and D. Lenschow, 2009: Attenuation of scalar fluxes measured with spatially displaced sensors. *Bound.-Layer Meteor.*, **130**, 275–300.
- Kaimal, J., J. Wyngaard, Y. Izumi, and O. Coté, 1972: Spectral characteristics of the surface-layer turbulence. *Quart. J. Roy. Meteor. Soc.*, **98**, 563–589.
- Kristensen, L., J. Mann, S. Oncley, and J. Wyngaard, 1997: How close is close enough when measuring scalar fluxes with displaced sensors? *J. Atmos. Oceanic Technol.*, **14**, 814–821.
- Laubach, J., and K. McNaughton, 1998: A spectrum-independent procedure for correcting eddy fluxes measured with separated sensors. *Bound.-Layer Meteor.*, **89**, 445–467.
- Lee, X., and T. Black, 1994: Relating eddy correlation sensible heat flux to horizontal sensor separation in the unstable atmospheric surface layer. *J. Geophys. Res.*, **99**, 18 545–18 553.
- Lumley, J., and H. Panofsky, 1964: *The Structure of Atmospheric Turbulence*. Wiley, 239 pp.
- Moore, C., 1986: Frequency response corrections for eddy correlation systems. *Bound.-Layer Meteor.*, **37**, 17–35.
- Nicholls, S., and C. Readings, 1981: Spectral characteristics of the surface-layer turbulence over sea. *Quart. J. Roy. Meteor. Soc.*, **107**, 591–614.

- OHATS, cited 2009: Ocean Horizontal Array Turbulence Study (OHATS). [Available online at <http://www.who.edu/science/AOPE/dept/OHATS/intro.html>.]
- Ruppert, J., C. Thomas, and T. Foken, 2006: Scalar similarity for relaxed eddy accumulation methods. *Bound.-Layer Meteor.*, **120**, 39–63.
- Sahlée, E., A.-S. Smedman, U. Högström, and A. Rutgersson, 2008: Reevaluation of the bulk exchange coefficient for humidity at sea during unstable and neutral conditions. *J. Phys. Oceanogr.*, **38**, 257–272.
- Smedman, A.-S., U. Högström, E. Sahlée, and C. Johansson, 2007: Critical re-evaluation of the bulk transfer coefficient for sensible heat over the ocean during unstable and neutral conditions. *Quart. J. Roy. Meteor. Soc.*, **133**, 227–250.
- Sullivan, P., J. Edson, T. Horst, J. Wyngaard, and M. Kelly, 2006: Subfilter scale fluxes in the marine surface layer: Results from the Ocean Horizontal Array Turbulence Study (OHATS). Preprints, *17th Symp. on Boundary Layers and Turbulence*, San Diego, CA, Amer. Meteor. Soc., 4.1. [Available online at http://ams.confex.com/ams/BLTA/AGFBioA/techprogram/paper_110884.htm.]
- Villalobos, F., 1997: Correction of eddy covariance water vapour flux using additional measurements of temperature. *Agric. For. Meteorol.*, **88**, 77–83.
- Wyngaard, J., and O. Coté, 1972: Cospectral similarity in the atmospheric surface layer. *Quart. J. Roy. Meteor. Soc.*, **98**, 590–603.